


Influence of PWM modulations on the DC-Link capacitor power losses of multiphase VSIs

Ander DeMarcos , Unai Ugalde , Jon Andreu , Markel Fernandez , Endika Robles 
 Universidad del País Vasco/Euskal Herriko Unibertsitatea (UPV/EHU)

e-mail: ander.demarcosa@ehu.eus

www.ehu.eus/es/web/apert

Abstract—In traction applications, particularly in transport electrification, multiphase drives are increasingly being an interesting alternative over their three-phase counterparts due to a range of advantages outweighing the additional cost, e.g. smoother torque performance, higher current capability, enhanced fault tolerance, higher efficiency and lower DC-Link current ripples. This work focuses on the impact this multiphase drives modulated by continuous and discontinuous PWM techniques have in a such a pricey and bulky component as it is the DC-Link capacitor. Taking into account that the equivalent series resistance of the DC-Link capacitor varies with frequency, the typical approximated calculation of the power losses in this component by means of the RMS value of the current is often inaccurate. Therefore, the spectral analysis of the DC-Link current has been carried out for the five-phase two-level VSI in order to estimate more accurately the power losses in the DC-Link capacitor and see which PWM modulation technique benefits this bulky and expensive component depending on its ESR curve and the selected switching frequency.

Index Terms—Multiphase, DC-Link capacitor, DC-Link current spectrum, PWM modulation, ESR, power loss.

I. INTRODUCTION

Multiphase systems, provides several advantages at an affordable cost compared with the classic three-phase electric motor driven systems (EMDS): power splitting between phases (lower currents and power losses through the inverter’s semiconductors for the same rated output power), reduction of the torque ripple (efficiency improvement), torque density improvement using harmonic current injection (in concentrated winding machines), lower DC-Link current ripples, and intrinsic fault-tolerant operation [1]–[4]. For these reasons, multiphase voltage-source inverters (VSIs) have great potential in life-critical applications, and when high power density is needed, such as in electric vehicle (EV) drivetrains, and aerospace applications [5]. In this context, as far as the multiphase topologies is concerned, the two-level star connected five-phase inverter (Fig. 1) is generally preferred among the multiphase topologies alternatives [6] since it provides a good trade-off among the system complexity, its cost, and the advantages mentioned above.

Pulse-width modulation (PWM) has become the standard when it comes to modulate these multiphase systems. They follow the same pattern or philosophy as the classic three-phase VSIs which have been extrapolated to higher number of phases system. Conceptually, there are two different strategies for carrying out pulse width modulation: Carrier-Based PWM (CB-PWM) and Space Vector PWM (SV-PWM). The first one consist of obtaining the semiconductor switching logic signals

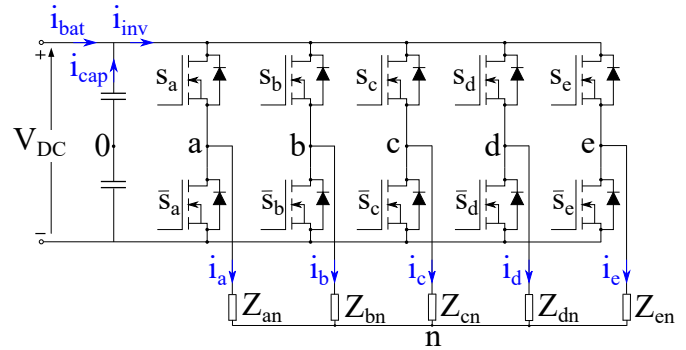


Fig. 1. Five-phase two-level star-connected VSI.

(Fig. 1, $s_a \dots s_e$) by comparing the normalized reference voltage signals ($v_a^* \dots v_e^*$), which act as modulator signals, with a triangular carrier (v_{cr}). On the other hand, SV-PWM consists of synthesizing a reference space vector (\vec{v}^*) by means of the instantaneous application of the possible states of the VSI, which are represented as vectors [7].

The choice of the modulation technique affect directly in many different manners the performance of the EMDS. One of the affected elements is the DC-Link capacitor, which is one of the most critical component of the converter. According to [8] almost 30% of the failures of the inverter are caused by this critical element. The lifetime of this component depends strongly on its hot-spot temperature and, consequently, on the current flowing through it and its equivalent serial resistor (ESR). In [9]–[11] it is analysed the RMS current of the DC-Link capacitor in five-phase systems. However, in [12]–[14] it is shown that although the RMS DC-Link capacitor current is an important parameter so as to quantify the power losses in the capacitor, as the ESR varies against the frequency, it is convenient to obtain the full DC-Link capacitor current spectrum. In this context, in [12]–[16] it is obtained the DC-Link capacitor current spectrum for three-phase systems, and in [17] for multiphase systems (but only for sinusoidal PWM modulation technique). Once the full harmonic spectrum is obtained, in [18] the power losses have been estimated for a traditional continuous PWM modulation in three-phase VSIs.

This paper analyses the DC-Link current spectrums for different CB-PWM in five-phase VSIs by means of the Fourier integral method. These current spectrums are used to estimate accurately the DC-Link capacitor power losses using the capacitor’s ESR curve. This way, it is quantified the errors which are usually made by using the typical approximation of

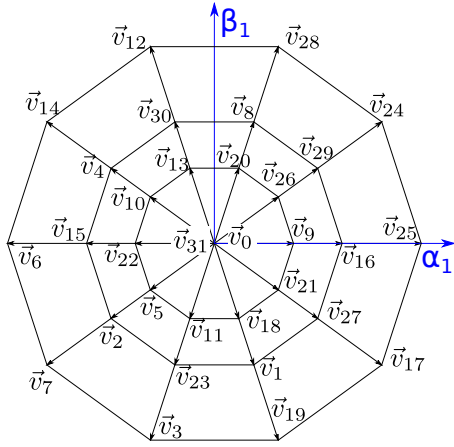


Fig. 2. Vectorial representation of the five-phase two-level star-connected VSI (plane $\alpha_1\beta_1$).

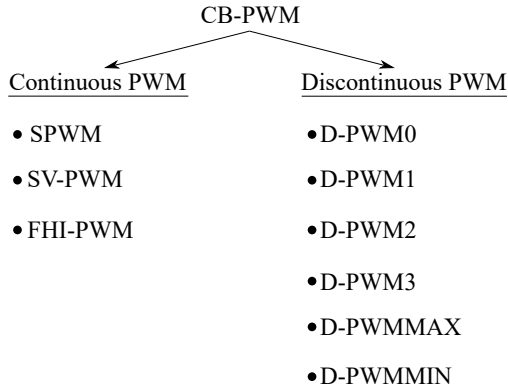


Fig. 3. Analysed single CB-PWM modulations analysed in this work.

the estimation of power losses of this component.

II. PWM MODULATION DEFINITION IN FIVE-PHASE VSIS.

Five-phase two-level star connected VSI (Fig. 1) can be vectorially represented with two orthogonal planes $\alpha_1\beta_1$ and $\alpha_3\beta_3$ in addition to the homopolar component [7]. As each switch of the five-phase inverter has two different states (ON/OFF), there are 2^5 possible states for the inverter's output voltage. These states are represented as 32 vectors which form three concentric decagons for each plane (Fig. 2). Under this vectorial approach, the vectors \vec{v}_1 to \vec{v}_{30} are active vectors and \vec{v}_0 and \vec{v}_{31} are zero vectors. In addition, according to the magnitude of the vectors in $\alpha_1\beta_1$ plane, there are three different vector groups: large vectors (L, situated in the outer decagon), middle vectors (M, middle decagon) and small vectors (S, inner decagon) (Fig. 2).

The inverter's states which have been obtained by the single carrier¹ based PWM modulation algorithms can be represented vectorially in the $\alpha_1\beta_1$ plane as 2L, 2M and zero vectors².

¹The carrier frequency is the same as the switching frequency ($f_{cr} = f_{sw}$).

²These PWM modulation techniques are known as 2L2M PWM.

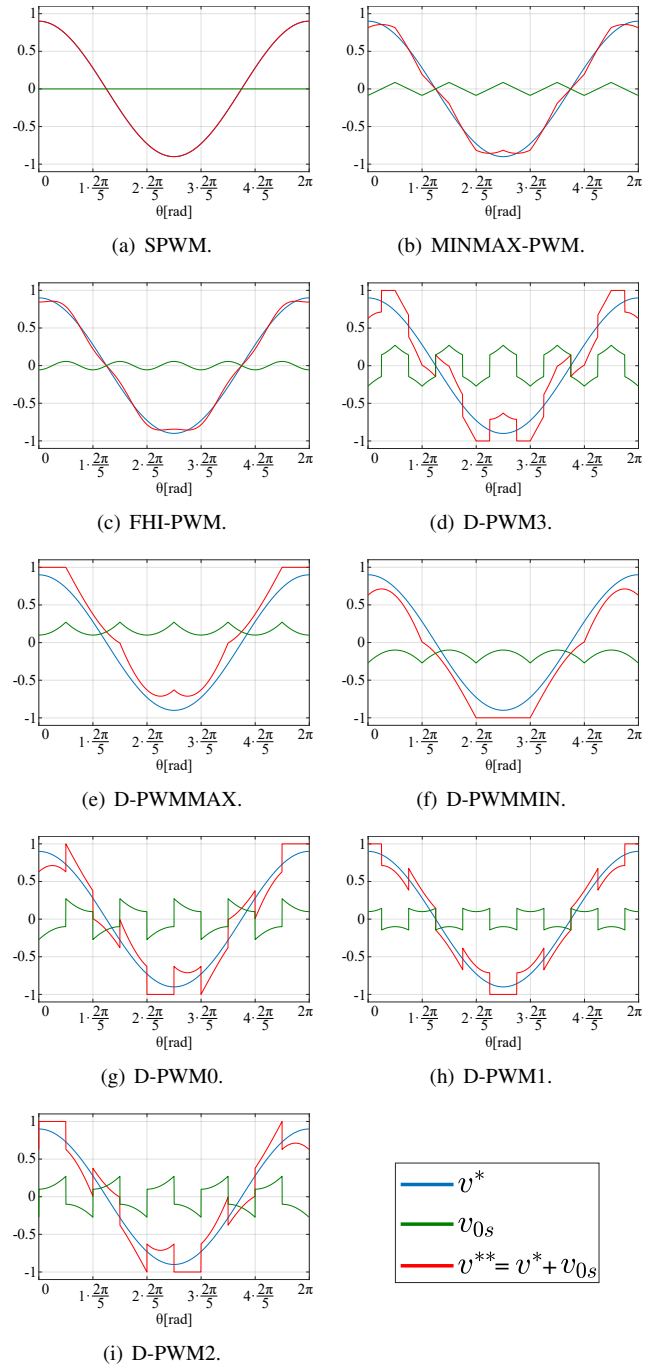


Fig. 4. Modulating and zero-sequence components for continuous and discontinuous CB-PWM techniques using $M = 0.9$.

Depending on the desired output voltage amplitude, which is proportional to the modulation index of the inverter, the duty cycles of the active vectors are set [7]. However, there is a degree of freedom when it comes to manage the zero vectors which leads to different PWM modulation techniques (Fig. 3). During both zero vector states (t_0 and t_{31}) the input current of the inverter (i_{inv}) is zero, therefore these CB-PWM modulation techniques give the same input RMS current.

The different CB-PWM modulation techniques are obtained by means of the injection of different zero-sequence components (v_{0s} , which are multiples of the 5th harmonic) into the reference signals (v^*) (Fig. 4). In this context, the CB-PWM modulations can be in turn subdivided between continuous and discontinuous modulations [7]. On the one hand, sinusoidal PWM (SPWM), 5th harmonic injection PWM (FHI-PWM) and min-max method PWM (MINMAX-PWM, sometimes also known as SV-PWM), are known as continuous modulations (C-PWM) (Fig. 3). All of these continuous PWM use both zero states (t_0 and t_{31}). On the other hand, D-PWM0, D-PWM1, D-PWM2, D-PWM3, D-PWMMAX and D-PWMMIN are known as discontinuous modulations (D-PWM) (Fig. 3) because they use a single zero state, and consequently, one branch does not switch in a whole switching period (when v^{**} is clamped to ± 1 in Fig. 4) [7]. This fact leads to a significant reduction of the switching power losses in the semiconductors of the VSI for discontinuous PWM techniques because the average equivalent switching frequency is reduced to $4/5 \cdot f_{sw}$ due to the fact that there are only switching four branches out of five.

The vast majority of modulation techniques, including the mentioned CB-PWM, are primarily aimed at synthesising high quality (low THD) output current. On the other hand, some of them have partial objectives improving other figures of merit such as reducing the switching losses and reducing the common-mode voltage. However, these modulations rarely focus on achieving lower inverter input current ripple and spectrum. Considering how this input current spectrum affects via the power losses in the temperature and consequently, in the lifetime of such bulky and expensive component as it is the DC-Link capacitor, it is interesting to analyse the influence of the different CB-PWM modulation techniques in this aspect.

III. APPROXIMATED POWER LOSS ESTIMATION IN THE DC-LINK CAPACITOR

The classical way to obtain the power losses in the DC-Link capacitor is defined by:

$$P_{loss} = ESR \cdot I_{cap,RMS}^2, \quad (1)$$

where ESR is the equivalent serial resistance of this capacitor, which is considered constant in the whole frequency range (usually taken at f_{sw}) and $I_{cap,RMS}$ is the RMS value of the current through the DC-Link capacitor.

Applying Kirchoff in Fig. 1, it is deduced:

$$\dot{i}_{inv} = \dot{i}_{cap} + \dot{i}_{bat}. \quad (2)$$

Assuming that the whole current ripple of the inverter input comes from the DC-Link capacitor ($\dot{i}_{cap} = \dot{i}_{inv,AC}$) and the battery supplies the whole average current of the inverter ($I_{bat} = I_{inv,avg}$), it is deduced:

$$I_{cap,RMS}^2 = I_{inv,RMS}^2 - I_{inv,avg}^2. \quad (3)$$

Performing a power balance between inverter's input and output it is deduced that [19]:

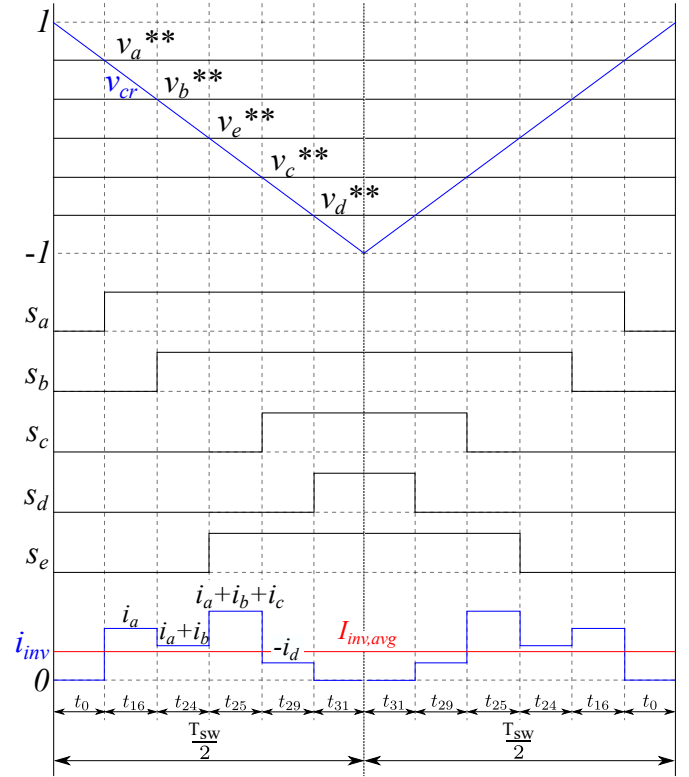


Fig. 5. Typical inverter's input current waveform for CB-PWM modulations.

$$I_{inv,avg} = \frac{5M}{4} \hat{I}_o \cos \phi, \quad (4)$$

where M is modulation index, ϕ is the current phase angle, and \hat{I}_o is the output peak current value.

On the other hand, in [9], analysing the different subintervals of Fig. 5, and assuming that the output current has no ripple, and that the switching frequency (f_{sw}) is much higher than the fundamental reference voltage frequency (f_1), the following compact expression of $I_{inv,rms}$ is obtained:

$$I_{inv,RMS} = \sqrt{\frac{5}{2\pi} M \hat{I}_o^2 \left[\frac{4}{3} \cos^2 \phi \left(\sin \frac{2\pi}{5} + \sin \frac{\pi}{5} \right) + \frac{2}{3} \left(2 \sin \frac{\pi}{5} - \sin \frac{2\pi}{5} \right) \right]}. \quad (5)$$

Substituting (4) and (5) in (3), the final expression of $I_{cap,RMS}$ is obtained:

$$I_{cap,RMS} = \sqrt{\frac{\hat{I}_o^2 M}{2\pi} \left\{ \cos^2 \phi \left[\frac{20}{3} \left(\sin \frac{2\pi}{5} + \sin \frac{\pi}{5} \right) - \frac{25\pi}{8} M \right] + \frac{10}{3} \left(2 \sin \frac{\pi}{5} - \sin \frac{2\pi}{5} \right) \right\}} \quad (6)$$

where it can be deduced that $I_{cap,RMS}$ does not depend on the modulation technique³. This happens because both zero states (t_0 and t_{31} in Fig. 5) have the same inverter input current value, which means the distribution of these zero states does

³Referring to the modulation techniques analysed in this work (traditional 2L2M continuous and discontinuous PWM modulation techniques).

not affect on this parameter. As it can be observed in (6), the RMS current through the capacitor depends on M , ϕ , and \hat{I}_o .

However, in real cases, and taking into account that the ESR varies with frequency, a more complex model, where it is necessary to know the harmonic spectrum, has to be applied so as to estimate more accurately the power losses of the DC-Link capacitor:

$$P_{loss} = \sum_{h=1}^{\infty} [ESR(f_h) \cdot I_{cap,h,RMS}^2], \quad (7)$$

where h is the harmonic order, $ESR(f_h)$ is the equivalent series resistance of the DC-Link capacitor for the h harmonic, and $I_{cap,h,RMS}$ is the RMS value of the h harmonic of the DC-Link capacitor's current.

IV. DOUBLE FOURIER INTEGRAL ANALYSIS OF A TWO-LEVEL PWM WAVEFORM

PWM switched waveforms are function of two time periodic independent variables $f(x, y)$: the carrier waveform $x(t) = \omega_{cr}t$ and reference or modulating waveform $y(t) = \omega_0t = \theta$. In [14] it is shown how a Fourier series expression is obtained and developed for this double variable controlled waveform $f(x, y)$:

$$\begin{aligned} f(x, y) &= \frac{A_{00}}{2} + \sum_{n=1}^{\infty} [A_{0n} \cos(ny) + B_{0n} \sin(ny)] \\ &+ \sum_{m=1}^{\infty} [A_{m0} \cos(mx) + B_{m0} \sin(mx)] \\ &+ \sum_{m=1}^{\infty} \sum_{\substack{n=-\infty \\ (n \neq 0)}}^{\infty} [A_{mn} \cos(mx + ny) + B_{mn} \sin(mx + ny)], \end{aligned} \quad (8)$$

where the Fourier coefficients A_{mn} and B_{mn} can be grouped in \bar{C}_{mn} as:

$$\bar{C}_{mn} = A_{mn} + jB_{mn} = \frac{1}{2\pi^2} \int_{-\pi}^{\pi} \int_{-\pi}^{\pi} f(x, y) e^{j(mx+ny)} dx dy, \quad (9)$$

where m is the carrier index variable and n is the baseband index variable. These two variables (m, n) define the frequency of each harmonic component as $\omega = m\omega_{cr} + n\omega_0$.

There are two main ways for the determination of the harmonic frequency components C_{mn} : the Fast Fourier Transform (FFT) and the Double Fourier integral analysis. While the FFT requires a completely sampled signal and its mathematical development, the Double Fourier integral analysis provides a more simple and compact way for obtaining these harmonic components [12], [18].

When the Fourier analysis is carried out for the current of one branch of the inverter ($i_{inv,a}$, Fig. 1), it has to be considered that $f(x, y)$ are some rectangular pulses (assuming that $\omega_c \gg \omega_0$):

$$f(x, y) = \begin{cases} 0 & \text{if } v^{**} \leq v_{cr} \\ \hat{I}_o \cos(y - \phi) & \text{if } v^{**} > v_{cr} \end{cases} \quad (10)$$

This way, the Fourier coefficients C_{mn} follow the next double Fourier integral:

$$\bar{C}_{mn} = \frac{\hat{I}_o}{2\pi^2} \int_0^{2\pi} \left(\int_{-\frac{\pi}{2}(1+v^{**}(y))}^{\frac{\pi}{2}(1+v^{**}(y))} \cos(y - \phi) \cdot e^{j(mx+ny)} dx \right) dy \quad (11)$$

It can be observed in (11) that the Fourier coefficients, and in consequence, the current spectrum of $i_{inv,a}$, does depend on the PWM technique by the inner integral's limits $v^{**}(y)$.

Similarly, the Fourier analysis of the input current through the other branches must be obtained and their effects added in order to obtain the full current harmonic spectrum of i_{inv} . The input current waveform of the consecutive branch of an equilibrated two-level five-phase inverter is analogous to the input current of the previous branch but shifted an angle of $2\pi * n/5$ rad. For example, the Fourier coefficients of the branch 'b' can be obtained by taking as a reference the coefficient corresponding to the branch 'a' and multiplying it by the complex number $1 \cdot e^{(j \cdot 2\pi * n/5)}$. Thus, the Fourier coefficients of the total input current of the inverter are obtained by the complex sum of the coefficients of every single branch of the inverter.

V. INPUT CURRENT AND DC-LINK CAPACITOR POWER LOSS SPECTRAL ANALYSIS

A. CB-PWM modulation techniques in a five-phase VSI

Applying the Fourier double integral analysis of Section IV, the different current spectrums of traditional single CB-PWM modulations have been obtained with the phase angle $\phi = 0$ rad (Fig. 6). For continuous modulations, the following can be observed:

- Predominant harmonic component is at $2f_{sw}$ ($m = 2$ and $n = 0$). It has a maximum point at $M \approx 0.6$.
- MINMAX-PWM and FHI-PWM are quite equivalent in the full range of frequency and modulation index.
- SPWM has smaller sideband harmonics at $m = 1$ and $n \pm 5$ than MINMAX-PWM and FHI-PWM.

Regarding to discontinuous modulations:

- All analysed discontinuous PWM modulations have a significant harmonic component around f_{sw} ($m = 1$).
- D-PWMMAX and D-PWMMIN are almost equivalent. The sideband harmonics around $m = 1$ are almost insignificant and the predominant component is at $m = 1$ and $n = 0$.
- D-PWM0, D-PWM1, D-PWM2, and D-PWM3 are almost equivalent. They have wide sideband harmonics around $m = 1$, which leads to have harmonic components at lower frequencies.

B. Comparison between a five-phase and a three-phase VSI for the SPWM modulation technique.

In order to perform a comparison between two inverters in which the phase number is not the same as far as the input current spectrum is concerned, it has been set the same output

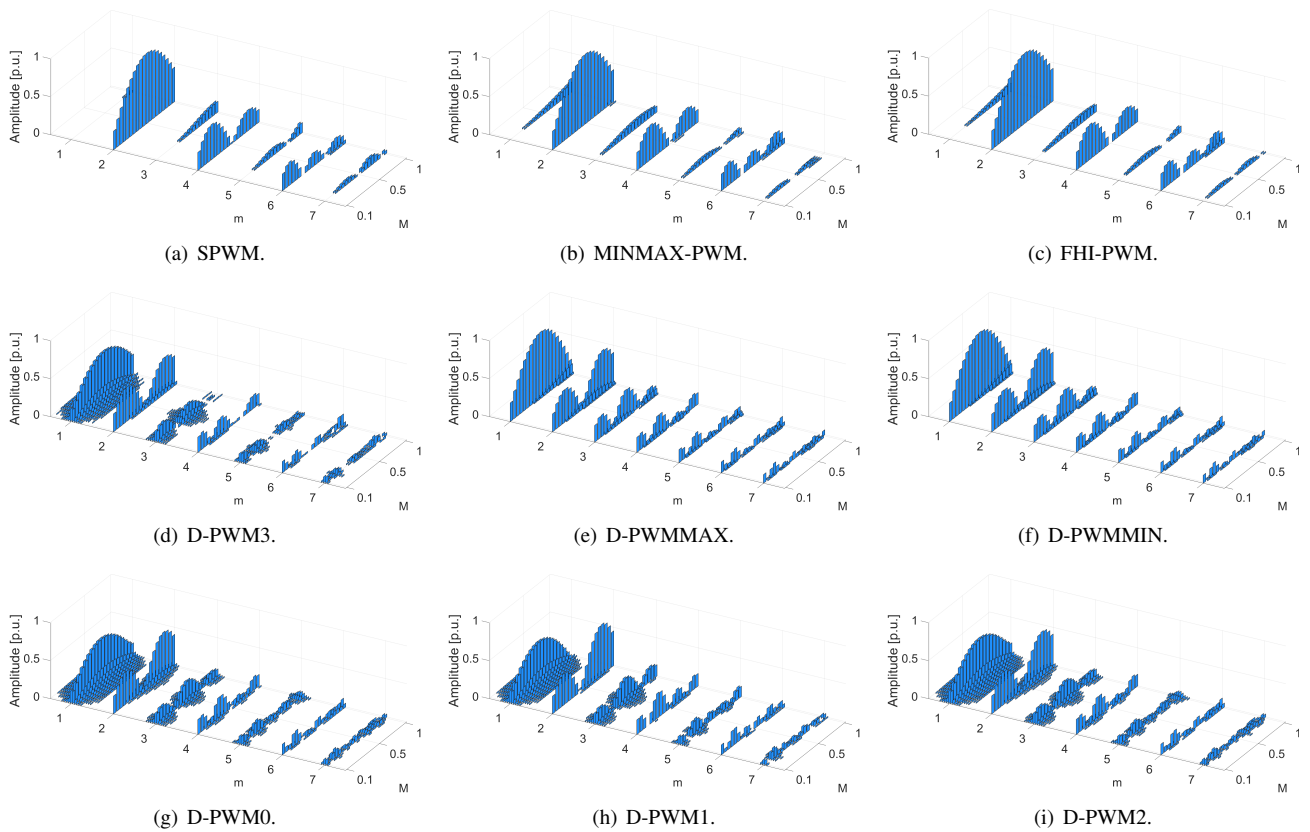


Fig. 6. Amplitudes of the input current harmonic spectrum for the analysed CB-PWM modulations with $\phi = 0 \text{ rad}$.

power for both VSIs. This means that the peak value of the phase current in a three-phase systems is $5/3$ times higher than in a five-phase systems for the same output power.

$$\hat{I}_{o,3ph} = \frac{5}{3} \hat{I}_{o,5ph} \quad (12)$$

In Fig. 7 it is compared the inverter's input current spectrum of a five-phase inverter and a three-phase inverter for SPWM modulation. Here it can be observed that while in three-phase VSIs the sideband harmonics exist at $m = 1, n = \pm 3$, in five-phase VSIs exist at $m = 1, n = \pm 5$. In addition, these harmonic amplitudes are reduced significantly as the number of phases is increased. Since the harmonics of the input current have smaller amplitudes in a higher phase number system, the input current's RMS value will be reduced. Consequently, the RMS value of the DC-Link capacitor's current will be also reduced [20].

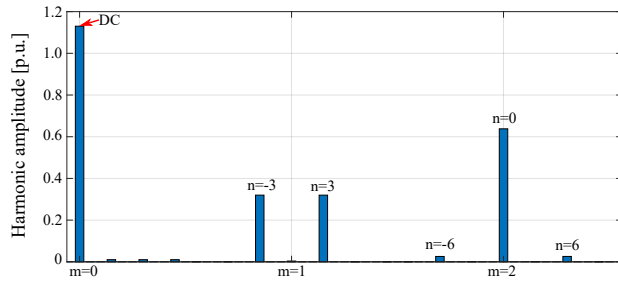
C. DC-Link capacitor power losses: spectral analysis

In order to estimate the power losses through the DC-Link, it has been selected polypropylene metallized film (MKP) capacitor for automotive applications B25632E1117K000 ($110 \mu\text{F}$, 1000 VDC) from TDK Electronics. The variation of ESR with the frequency can be observed in Fig. 8.

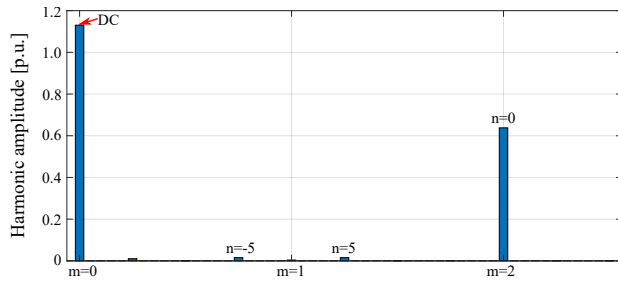
There have been performed two analysis with different switching frequencies (1 kHz and 10 kHz) in order to see the influence of this parameter in the power losses of the selected

capacitor. In Fig. 9 the DC-Link power losses for different PWM modulation techniques relative to SPWM power losses can be observed so as to make a comparison among them. Here, it can be observed that for $f_{sw} = 10 \text{ kHz}$ (Fig. 9(a)) the analysed PWM modulation techniques (Fig. 3) obtain a similar result regarding the DC-Link capacitor power losses. This happens because for this $f_{sw} = 10 \text{ kHz}$ case the ESR of the capacitor is almost constant in the frequency range where the inverter's input current has its predominant harmonics (around $m = 1$, and $m = 2$). On the other hand, when the analysis is carried out at $f_{sw} = 1 \text{ kHz}$ (Fig. 9(b)), as the ESR curve goes down with frequency in that area, the modulations which have a predominant component at smaller frequencies such as discontinuous modulations which have $m = 1$ as a predominant component, have a worst performance (higher P_{loss}) than continuous PWM modulation techniques. These greater power losses are harmful for the lifetime of the capacitor.

In Fig. 10 it has been compared the power losses calculated by the full spectral analysis of (7) and the ones calculated by the approximation of (1) where the ESR has been considered as constant ($ESR = ESR@f_{sw}$). The comparison performed at 10 kHz in Fig. 10(a) shows that as the ESR curve is almost constant around the frequencies where i_{inv} has its predominant harmonics, it is an acceptable approximation where the error is small enough. However, when it comes to switch at 1 kHz



(a) Three-phase VSI.



(b) Five-phase VSI.

Fig. 7. Input current spectrum comparison between a two-level five-phase VSI and a two-level three-phase VSI for SPWM modulation with $M = 0.9$ $\phi = 0$ rad.

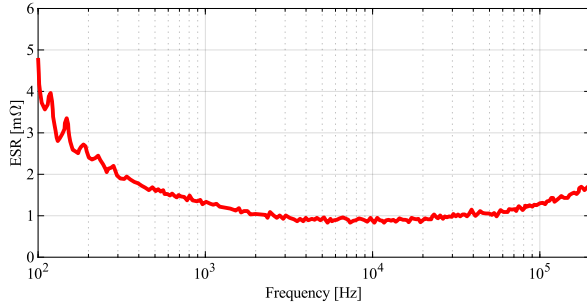
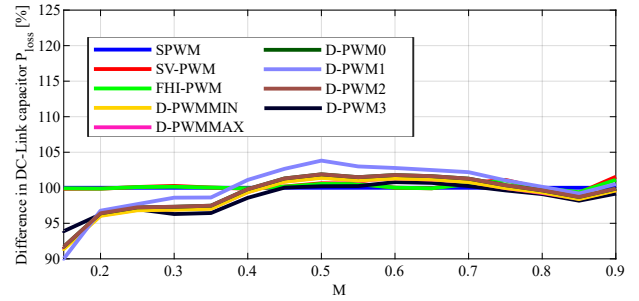
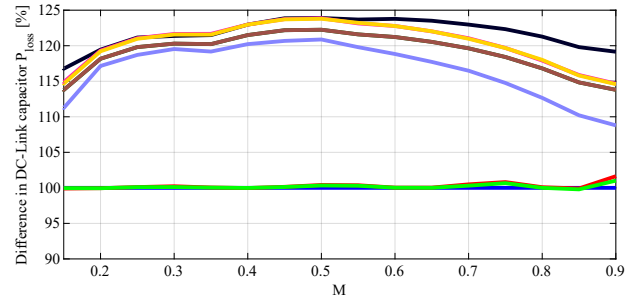


Fig. 8. ESR of the DC-Link capacitor TDK MKP B25632E1117K000.

(Fig. 10(b)), as the ESR is not constant around the frequencies where i_{inv} has its predominant harmonics, this approximation is not good enough and should not be used. On the other hand, for this specific cases where the ESR of the capacitor goes down with the frequency (at $f_{sw} = 1$ kHz), the estimated power losses would be always overestimated because in this approximation it would be used the highest ESR value ($ESR@f_{sw}$) for obtaining the power losses. In addition, as in continuous modulations it predominates the $m = 2$ carrier wave harmonic and in discontinuous modulations it does $m = 1$ as well as $m = 2$, the error made by using the approximated expression for continuous would be bigger than for discontinuous modulations because the used ESR values would be lower.



(a) $f_{sw} = 10$ kHz.



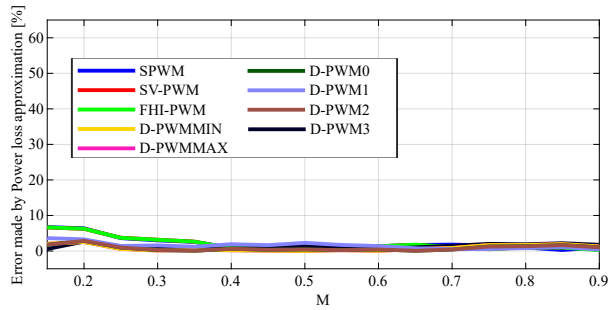
(b) $f_{sw} = 1$ kHz.

Fig. 9. Difference of the DC-Link power losses for the analysed PWM modulations compared to SPWM with $\phi = 0$ rad for two different switching frequencies.

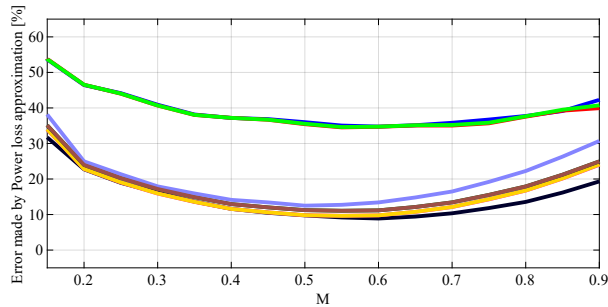
VI. CONCLUSIONS

This work has been focused on a such critical element of the CB-PWM modulated multiphase VSIs as it is the DC-Link capacitor. It has been proved that as the number of phases increases, the current ripple harmonic is reduced benefiting the lifetime of this element. As far as the analysed CB-PWM modulation techniques are concerned, it has been seen that there are some predominant components around the carrier wave harmonics $m = 1$ and $m = 2$. More precisely, continuous modulations have a significant predominant carrier wave harmonics at $m = 2$ and discontinuous modulation techniques have a wide sideband around $m = 1$ even though it cannot be neglected their carrier wave harmonics at $m = 2$ (it is also predominant even though it is smaller than continuous).

The analysed CB-PWM modulations can provide different power losses in the DC-Link capacitor even though all of them have the same RMS current. This happens due to the fact that every single PWM modulation have a different current waveform in the inverter's input, and in consequence, different harmonic spectrum. This current spectrum is critical in order to estimate the power losses through the DC-Link because of the dependency of its ESR with the frequency. As it has been seen, for the specific capacitor and switching frequencies analysed in this paper, performing the typical approximation so as to estimate the power losses in the DC-Link capacitor can provoke unacceptable relative errors up to 50%. However, the importance of the current spectrum analysis in the DC-Link so as to calculate the power losses can be neglected if the



(a) $f_{sw} = 10$ kHz.



(b) $f_{sw} = 1$ kHz.

Fig. 10. Relative error between the DC-Link power losses calculated with the whole spectrum and with the approximation with $\phi = 0$ rad for two different switching frequencies.

ESR curve is almost constant around the switching frequency. Thus, knowing the switching frequency and the ESR curve is important to know whether the power loss approximation or input current spectrum based calculation should be carried out.

VII. ACKNOWLEDGEMENTS

This work has been supported in part by the Government of the Basque Country within the fund for research groups of the Basque University system IT978-16 and the research program ELKARTEK (project ENSOL2-KK-2020/00077) and the MCIN/AEI/10.13039/501100011033 within the project PID2020-115126RB-I00, as well as the support of the UPV/EHU pre-doctoral programme (PIF20-305).

REFERENCES

- [1] E. Levi, "Advances in converter control and innovative exploitation of additional degrees of freedom for multiphase machines," *IEEE Transactions on Industrial Electronics*, vol. 63, no. 1, pp. 433–448, 2016.
- [2] W. N. W. A. Munim, M. J. Duran, H. S. Che, M. Bermúdez, I. González-Prieto, and N. A. Rahim, "A unified analysis of the fault tolerance capability in six-phase induction motor drives," *IEEE Transactions on Power Electronics*, vol. 32, no. 10, pp. 7824–7836, 2017.
- [3] X. Wang, Z. Wang, Z. Xu, M. Cheng, W. Wang, and Y. Hu, "Comprehensive diagnosis and tolerance strategies for electrical faults and sensor faults in dual three-phase PMSM drives," *IEEE Transactions on Power Electronics*, vol. 34, no. 7, pp. 6669–6684, 2019.
- [4] G. Feng, C. Lai, M. Kelly, and N. C. Kar, "Dual three-phase PMSM torque modeling and maximum torque per peak current control through optimized harmonic current injection," *IEEE Transactions on Industrial Electronics*, vol. 66, no. 5, pp. 3356–3368, 2019.
- [5] E. Robles, M. Fernandez, J. Andreu, E. Ibarra, and U. Ugalde, "Advanced power inverter topologies and modulation techniques for common-mode voltage elimination in electric motor drive systems," *Renewable and Sustainable Energy Reviews*, vol. 140, no. 110746, pp. 1–26, 2021.

- [6] E. Robles, M. Fernandez, J. Andreu, E. Ibarra, J. Zaragoza, and U. Ugalde, "Common-mode voltage mitigation in multiphase electric motor drive systems," *Renewable and Sustainable Energy Reviews*, vol. 157, no. 111971, pp. 1–21, 2022.
- [7] J. Prieto, M. Jones, F. Barrero, E. Levi, and S. Toral, "Comparative analysis of discontinuous and continuous PWM techniques in VSI-fed five-phase induction motor," *IEEE Transactions on Industrial Electronics*, vol. 58, no. 12, pp. 5324–5335, 2011.
- [8] U. Choi, F. Blaabjerg, and K. Lee, "Study and handling methods of power IGBT module failures in power electronic converter systems," *IEEE Trans. on Power Electronics*, vol. 30, no. 5, pp. 2517–2533, 2015.
- [9] P. A. Dahono, Deni, C. P. Akbarifutra, and A. Rizqiawan, "Input ripple analysis of five-phase pulse width modulated inverters," *IET Power Electronics*, vol. 3, no. 5, pp. 716–723, 2010.
- [10] P. A. Dahono, Deni, and A. Rizqiawan, "Analysis and minimization of input current and voltage ripples of five-phase PWM inverters," in *Proc. of the International Power and Energy Conference (PECON)*, 2008, pp. 625–629.
- [11] J. Kolar and S. Round, "Analytical calculation of the RMS current stress on the dc-link capacitor of voltage-PWM converter systems," *Electric Power Applications*, vol. 153, no. 4, pp. 535 – 543, 2006.
- [12] M. H. Bierhoff and F. W. Fuchs, "DC-Link harmonics of three-phase voltage-source converters influenced by the pulsewidth-modulation strategy - An analysis," *IEEE Transactions on Industrial Electronics*, vol. 55, no. 5, pp. 2085–2092, 2008.
- [13] B. P. McGrath and D. G. Holmes, "A general analytical method for calculating inverter DC-Link current harmonics," *IEEE Transactions on Industry Applications*, vol. 45, no. 5, pp. 1851–1859, 2009.
- [14] D. G. Holmes and T. A. Lipo, *Pulse Width Modulation for Power Converters: Principles and Practice*. Wiley-IEEE Press, 2003.
- [15] C. Rettner, G. Jacob, M. Schiedermeier, A. Apelsmeier, and M. März, "Voltage ripple analysis based on DC-Link current harmonics for voltage source inverters," in *Proc. of the Control and Modeling for Power Electronics (COMPEL)*, 2019, pp. 1–6.
- [16] N. Rouhana, N. Patin, G. Friedrich, E. Negre, and S. Loudot, "Analysis of DC-Link current harmonics for unconventional PWM strategies - application of the double Fourier integral method," in *Proc. of the European Conference on Power Electronics and Applications (EPE ECCE-Europe)*, 2015, pp. 1–8.
- [17] N. Kesbia, J.-I. Schanen, L. Garbuio, and H. Alawieh, "An analytical model of the DC-Link current ripple in multiphase PWM inverter," in *Proc. of the Power Electronics, Intelligent Motion, Renewable Energy and Energy Management (PCIM)*, 2020, pp. 1–5.
- [18] G. I. Orfanoudakis, S. M. Sharkh, and M. A. Yuratic, "Analysis of DC-Link capacitor losses in three-level neutral point clamped and cascaded h-bridge voltage source inverters," in *Proc. of the IEEE International Symposium on Industrial Electronics (ISIE)*, 2010, pp. 664–669.
- [19] S. M. Dabour, A. S. Abdel-Khalik, A. M. Massoud, and S. Ahmed, "Analysis of scalar PWM approach with optimal common-mode voltage reduction technique for five-phase inverters," *IEEE Journal of Emerging and Selected Topics in Power Electronics*, vol. 7, no. 3, pp. 1854–1871, 2019.
- [20] A. Muqorobin, P. A. Dahono, and A. Purwadi, "Optimum phase number for multiphase PWM inverters," in *Proc. of the International Conference on Electrical Engineering, Computer Science and Informatics (EECSI)*, 2017, pp. 1–6.